



**HAL**  
open science

# Theoretical prediction of Reynolds stresses and velocity profiles for barotropic turbulent jets

Eric Woillez, Freddy Bouchet

► **To cite this version:**

Eric Woillez, Freddy Bouchet. Theoretical prediction of Reynolds stresses and velocity profiles for barotropic turbulent jets . EPL - Europhysics Letters, 2017. hal-01357478v2

**HAL Id: hal-01357478**

**<https://hal.science/hal-01357478v2>**

Submitted on 7 Jul 2017

**HAL** is a multi-disciplinary open access archive for the deposit and dissemination of scientific research documents, whether they are published or not. The documents may come from teaching and research institutions in France or abroad, or from public or private research centers.

L'archive ouverte pluridisciplinaire **HAL**, est destinée au dépôt et à la diffusion de documents scientifiques de niveau recherche, publiés ou non, émanant des établissements d'enseignement et de recherche français ou étrangers, des laboratoires publics ou privés.

# Theoretical prediction of Reynolds stresses and velocity profiles for barotropic turbulent jets

E.WOILLEZ<sup>1</sup> and F.BOUCHET<sup>1</sup>

<sup>1</sup> *Univ Lyon, Ens de Lyon, Univ Claude Bernard, CNRS, Laboratoire de Physique, F-69342 Lyon, France*

PACS 47.27.eb – Statistical theories and models  
 PACS 47.10.-g – General theory in fluid dynamics  
 PACS 47.27.wg – Turbulent jets

**Abstract** –It is extremely uncommon to be able to predict the velocity profile of a turbulent flow. In two-dimensional flows, atmosphere dynamics, and plasma physics, large scale coherent jets are created through inverse energy transfers from small scales to the largest scales of the flow. We prove that in the limits of vanishing energy injection, vanishing friction, and small scale forcing, the velocity profile of a jet obeys an equation independent of the details of the forcing. We find another general relation for the maximal curvature of a jet and we give strong arguments to support the existence of an hydrodynamic instability at the point with minimal jet velocity. Those results are the first computations of Reynolds stresses and self consistent velocity profiles from the turbulent dynamics, and the first consistent analytic theory of zonal jets in barotropic turbulence.

Theoretical prediction of velocity profiles of inhomogeneous turbulent flows is a long standing challenge, since the nineteenth century. It involves closing hierarchy for the velocity moments, and for instance obtaining a relation between the Reynolds stress and the velocity profile. Since Boussinesq in the nineteenth century, most of the approaches so far have been either empirical or phenomenological. Even for the simple case of a three dimensional turbulent boundary layer, plausible but so far unjustified similarity arguments may be used to derive von Kármán logarithmic law for the turbulent boundary layer (see for instance [1]), but the related von Kármán constant [2] has never been computed theoretically. Still this problem is a crucial one and has some implications in most of scientific fields, in physics, astrophysics, climate dynamics, and engineering. Equations (6-7), (9), and (11) are probably the first prediction of the velocity profile for turbulent flows, and relevant for barotropic flows.

In this paper we find a way to close the hierarchy of the velocity moments, for the equation of barotropic flows with or without effect of the Coriolis force. This two dimensional model is relevant for laboratory experiments of fluid turbulence [3], liquid metals [4], plasma [5], and is a key toy model for understanding planetary jet formation [6] and basics aspects of plasma dynamics on Tokamaks in

relation with drift waves and zonal flow formation [7]. It is also a relevant model for Jupiter troposphere organization [8]. Moreover, our approach should have future implications for more complex turbulent boundary layers, which are crucial in climate dynamics in order to quantify momentum and energy transfers between the atmosphere and the ocean.

It has been realized since the sixties and seventies in the atmosphere dynamics and plasma communities that in some regimes two dimensional turbulent flows are strongly dominated by large scale coherent structures. Jets and large vortices are often observed in numerical simulations or in experiments, but the general mechanism leading to such an organization of the flow at large scales is subtle and far from being understood. For simplicity, we consider in this paper the case of parallel jets favored by the  $\beta$  effect, however without  $\beta$  effect both jets and vortices can be observed [4, 9, 10]. When a large scale structure is created by the flow, a quasilinear approach may be relevant. Such a quasilinear approach requires solving a coupled equation for the mean flow and the Lyapunov equation that describes the fluctuations with a Gaussian approximation, just like the Lenard–Balescu equation in plasma kinetic theory. Numerical approaches and theoretical analysis have been systematically developed for fif-

51 teen years in order to solve and study such quasilinear or  
 52 related approximations [6,11]. In a recent theoretical paper,  
 53 the range of validity of such an approach has been  
 54 established by proving the self consistency of the approxi-  
 55 mations of weak forcing and dissipation limit [12]. While  
 56 this work gave theoretical ground to the approach, explicit  
 57 formula for the Reynolds stress cannot be expected in gen-  
 58 eral. However, in a recent work [13], an expression for the  
 59 Reynolds stress has been derived from the momentum and  
 60 energy balance equations by neglecting the perturbation  
 61 cubic terms in the energy balance (this follows from the  
 62 quasilinear approach justification [12]), but also neglect-  
 63 ing pressure terms (not justified so far, see [14]). This ap-  
 64 proach surprisingly predicts a constant velocity profile for  
 65 the outer region of a large scale vortex in two dimensions  
 66 that does not depend on the detailed characteristics of the  
 67 stochastic forcing but only on the total energy injection  
 68 rate  $\epsilon$  expressed in  $\text{m}^2\text{s}^{-3}$ . Another analytic expression  
 69 for the Reynolds stress has also been derived in the par-  
 70 ticular case of a linear velocity profile  $U$  in [15]. For the  
 71 case of dipoles for the 2D Navier–Stokes equations, the pa-  
 72 pers [16,17] following a computation analogous to the one  
 73 given in [15], shows that if the vorticity is passively ad-  
 74 vected (the third term in equation (5) below is neglected),  
 75 then the expression for the Reynolds stress discussed in  
 76 [10] is recovered ([17] also discusses other interesting as-  
 77 pects related to parts of the flow for which this relation  
 78 is not correct). What are the criteria for the validity of  
 79 these results? Can we reconcile the different results giving  
 80 a full theoretical justification and extend these for more  
 81 general cases?

We start from the equations for a barotropic flow on a  
 periodic beta plane with stochastic forcing

$$\partial_t \mathbf{V} + \mathbf{V} \cdot \nabla \mathbf{V} = -r \mathbf{V} - \frac{1}{\rho} \nabla P + \beta_d y \begin{pmatrix} V_y \\ -V_x \end{pmatrix} + \sqrt{2\epsilon} \mathbf{f} \quad (1)$$

where  $\mathbf{V} := \begin{pmatrix} V_x \\ V_y \end{pmatrix}$  is the two dimensional velocity field  
 with  $\nabla \mathbf{V} = 0$ .  $r$  models a linear friction, and  $\mathbf{f}$  is a stochas-  
 tic force white in time, with energy injection rate  $\epsilon$ ,  $\beta_d$  is  
 the Coriolis parameter,  $y$  the north-south coordinate. Fol-  
 lowing [12] we choose time and space units such that the  
 mean kinetic energy is 1, and  $L_x = 1$ . The non dimen-  
 sional equations for the vorticity  $\Omega = \nabla \wedge \mathbf{V}$  are

$$\partial_t \Omega + \mathbf{V} \cdot \nabla \Omega = -\alpha \Omega - \beta V_y + \sqrt{2\alpha\eta} \quad (2)$$

82 where  $\eta = \nabla \wedge f$ , and  $\mathbf{V}$  denotes from now on the nondi-  
 83 mensional velocity. Now  $\alpha = L \sqrt{\frac{r^3}{\epsilon}}$  is a nondimensional  
 84 parameter although we will often refer to it as the “fric-  
 85 tion”.  $\beta = \sqrt{\frac{r}{\epsilon}} L^2 \beta_d$  is the nondimensional Coriolis param-  
 86 eter. Eq. (2) still has three nondimensional parameters,  
 87  $\alpha, \beta$  and  $K$ , the typical Fourier wavenumber where energy  
 88 is injected.

Neglecting the pressure and cubic terms in the energy  
 balance and enstrophy balance, it is straightforward to  
 obtain the Reynolds stress expression

$$\langle uv \rangle = \frac{\epsilon}{U'} \quad (3)$$

89 where  $U' = dU/dy$ . This generalizes the result obtained  
 90 for a vortex [13] to the case of a jet with mean velocity  
 91  $U$ . Is it possible to justify those hypothesis on theoretical  
 92 ground, uncover the validity range of (3), and to generalize  
 93 it? We note that detailed numerical studies of the energy  
 94 balanced has been discussed in several papers [10,18,19].

95 In order to derive eq. (3), the key idea is to use the al-  
 96 ready justified [12] quasilinear approximation in the limit  
 97 of small forces and friction (inertial regime,  $\alpha \ll 1$ ), and to  
 98 further consider the limit of small scale forcing ( $K \gg 1$ ),  
 99 with fixed  $\beta$ . In these limits, energy is injected at small  
 100 scale and is dissipated at the largest scale of the flow.  
 101  $\alpha \ll 1$  is the proper regime for most geophysical turbulent  
 102 flows, for instance for giant gaseous planets like Jupiter  
 103 [20,21], and many two dimensional or rotating turbulence  
 104 experiments. The small scale forcing limit  $K \gg 1$  is the  
 105 most common framework for turbulence studies (see for  
 106 ex. [14]) and relevant for Jupiter troposphere. Also, com-  
 107 puting the pressure from the Navier–Stokes equations in-  
 108 volves inverting a Laplacian. It is thus natural to expect  
 109 the pressure term to have a power expansion in the pa-  
 110 rameter  $\frac{1}{K}$ , and thus vanish in the limit of large  $K$ . The  
 111 main idea is then to separate the flow  $\mathbf{V}$  in two parts,

$$\mathbf{V}(\mathbf{r}, t) = U(y, t) \mathbf{e}_x + \begin{pmatrix} u(\mathbf{r}, t) \\ v(\mathbf{r}, t) \end{pmatrix}. \quad \text{The mean velocity}$$

112  $U(y) \mathbf{e}_x = \frac{1}{L_x} \int dx \mathbb{E}[\mathbf{V}(x, y)]$  called the *mean flow* or *zonal*  
 113 *flow*, is defined as both the zonal and stochastic average of  
 114 the velocity field. In the following, the bracket  $\langle \rangle$  will be  
 115 used for this zonal and stochastic average. We are left with  
 116 two coupled equations, one governing the dynamics of the  
 117 mean flow, the other one describing the evolution of ed-  
 118 dies. In the limit where  $\alpha$  is small, it has been proven that  
 119 fluctuations are of order  $\sqrt{\alpha}$  and thus it is self-consistent  
 120 to neglect nonlinear terms in the equation for fluctuations  
 121 [12]. Then one can justify [12] that, at leading order in  $\alpha$ ,  
 122 the full velocity field statistics are described by a quasi-  
 123 Gaussian field (the velocity field is not Gaussian, but the  
 124 marginals when the zonal flow is fixed are Gaussian, just-  
 125 ifying a posteriori a second order closure corresponding  
 126 to the quasilinear approximation). Using also the incom-  
 127 pressibility condition, we obtain the quasilinear model  
 128

$$\partial_t U = -\alpha [\partial_y \langle uv \rangle + U] \quad (4)$$

$$\partial_t \omega + U \partial_x \omega + (\beta - U'') v = -\alpha \omega + \eta \quad (5)$$

129 where we have introduced  $\omega = \partial_x v - \partial_y u = \Delta \psi$ , the  
 130 vorticity of the fluctuations. Eq. (4) shows that the typical  
 131 time scale for the evolution of the mean flow  $U$  is  $\frac{1}{\alpha}$  which  
 132 is, following our assumption  $\alpha \ll 1$ , much larger than the  
 133 time scale for the evolution of eddies. Using this time scale  
 134 separation, we will consider that  $U$  is a constant field in  
 135 the second Eq. (5), and we will always solve  $\omega(t)$  for a  
 136 given  $U$ . We follow the strategy:

- First we solve the linear Eq. (5) and compute the  
stationary distribution  $\langle \omega^2 \rangle$  as a functional of  $U$ .
- The enstrophy balance for the fluctuations allows us

to relate  $\langle \omega^2 \rangle$  to the divergence of the Reynolds stress tensor (see the Supplementary Material [22]).

- Last we can use this expression to close the first Eq. (4), and discuss possible stationary profiles  $U$ .

To reach the first objective, we take advantage of the asymptotic regimes  $\alpha \rightarrow 0$  and  $K \rightarrow \infty$ . When we take those two limits, it is natural to ask whether they commute or not, and which nondimensional parameter will govern the difference between  $\alpha \rightarrow 0$  first or  $K \rightarrow \infty$  first. Our asymptotic calculations show that the key parameter is the ratio between  $\frac{U''}{K}$  and  $\alpha$ . Taking the limit  $\alpha \rightarrow 0$  first amounts to saying that  $\frac{U''}{\alpha K}$  is very large.

We first take the limit  $K \rightarrow \infty$  while keeping  $\alpha$  small but finite. The idea is to write Eq. (5) in an integral form using the Green function of the Laplacian, and use the fact that the Green function decreases very fast when  $K$  is large, which implies that the evolution of the flow is local in space. At this stage of the calculation,  $\alpha$  is small but finite, and the expression for the Reynolds stress depends both on  $\alpha$  and on the properties of the stochastic forcing. The complete calculation is reported in the Supplementary Material [22]. We emphasize that as long as  $\alpha$  is kept finite, the Reynolds stress depends on the Fourier spectrum of the stochastic forcing  $\eta$ . The result shows that the Reynolds stress can be expressed analytically as

$$\langle uw \rangle = \frac{1}{2\alpha} \chi \left( \frac{U'}{2\alpha} \right), \quad (6)$$

where the explicit expression of  $\chi$  is a parametric integral, see [22]. The stationary profile  $U$  thus verifies  $\frac{U''}{2\alpha} \frac{1}{2\alpha} \chi' \left( \frac{U'}{2\alpha} \right) = -U$ , which can be integrated using a primitive  $X$  of the function  $x \rightarrow x\chi'(x)$  in

$$X \left( \frac{U'}{2\alpha} \right) + \frac{1}{2} U^2 = C, \quad (7)$$

where  $C$  is the integration constant. It is in itself remarkable that for some range of the parameters, the flow of the barotropic quasilinear model can be computed from a Newtonian equation like (7).

In Eq. (7),  $X$  plays the role of a potential as if the equation would describe a particle moving in a one-dimensional potential. The constant in the right-hand side is set by  $U'(0)$  and depending on the value of this constant, there can be one, two or three solutions as shown in Fig. (1). If  $C > X_{max}$ , there is one solution for which  $U$  never vanishes. As the total flow momentum is zero, such solutions with either  $U > 0$  or  $U < 0$  are not physical. If  $X_0 < C < X_{max}$ , there are three possible solutions, one is periodic, the other two diverge. The periodic solution corresponds to  $\frac{U'}{2\alpha}$  confined in the well of  $X$ . In that case the flow is periodic and the solution exchanges kinetic energy in the term  $\frac{1}{2} U^2$  with potential energy  $X \left( \frac{U'}{2\alpha} \right)$ . Outside the well, the solutions are diverging, one corresponds to an increasing  $U$  and the other to a decreasing  $U$ . A linear stability analysis of the periodic solution of (7) shows that

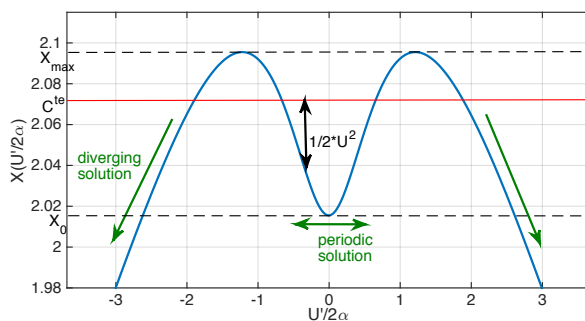


Fig. 1: In the limit of small scale forcing, the mean flow can be computed analytically from the Newtonian Eq. (7). We show here that the situation is analogous to a particle moving in a one-dimensional potential. The blue curve displays the potential  $X$  appearing in Eq.(7). If the constant of motion is less than  $X_{max}$ , there are two classes of solutions: the solution can be confined in the central well and is thus regular and periodic in space, or it is outside the well, and in this latter case it diverges.

this solution is unstable whereas the diverging solution is stable. Thus, the periodic regular solution is not a suitable candidate for the stationary mean velocity profile  $U(y)$ . If we now take the limit of vanishing  $\alpha$  in expression (6), a straightforward calculation using the explicit expression of  $\chi$  (given in [22]) allows us to recover expression (3) for the Reynolds stress because  $U' \langle uw \rangle \xrightarrow{\alpha \rightarrow 0} 1$  which is Eq. (3) with dimensional units. The physical interpretation of the limiting case (3) is very enlightening. The term  $U' \langle uw \rangle$  can be interpreted as the rate of energy transferred from small scale to large scale, therefore expression (3) is consistent: with the limit of large  $K$ , the evolution of eddies becomes local as if the perturbation only sees a region of width  $\frac{1}{K}$  around itself, and thus the different parts of the flow are decoupled. The other limit of small  $\alpha$  forces the energy to go to the largest scale to be dissipated because the dissipation at small scales becomes negligible.

Let us study the other limit where  $\alpha$  goes to zero first. The techniques used in this second case are very different than the previous one. We assume in this section that the linearized dynamics has no unstable modes. The calculation involves Laplace transform tools that were used in [23] to study the asymptotic stability of the linearized Euler equations. In the limit  $\alpha \ll 1$ , using [12], we derive in the Supplementary Material [22] the relation between the Reynolds stress divergence and the long time behavior of a disturbance  $\omega(y, 0)$  carried by a mean flow  $U(y)$ . This is an old problem in hydrodynamics, one has to solve the celebrated Rayleigh equation

$$\left( \frac{d^2}{dy^2} - k^2 \right) \varphi_\delta(y, c) + \frac{\beta - U''(y)}{U(y) - c - i\delta} \varphi_\delta(y, c) = \frac{\omega(y, 0)}{ik(U(y) - c - i\delta)}, \quad (8)$$

where  $\varphi_\delta(y, c) := \int_0^\infty dt \psi(y, t) e^{-ik(c+i\delta)t}$  is the Laplace transform of the stream function, and  $k$  is the  $x$ -component of the wavevector. The Laplace transform  $\varphi_\delta$  is well defined for any non zero value of the real variable

$\delta$  with a strictly negative product  $k\delta$ .  $c$  has to be understood as the phase speed of the wave, and  $k\delta$  is the (negative) exponential growth rate of the wave. Involved computations are then required to give the explicit expression of the Reynolds stress. Let us just mention that the difficulty comes from the fact that we have to take the limit  $\delta \rightarrow 0$  first in Eq. (8) before  $K \rightarrow \infty$ . Then we can relate  $\omega(y, \infty)$  to the Laplace transform  $\varphi_\delta$  taken at  $\delta = 0$ . The expression for the Reynolds stress in the inertial limit involves an integral with the profile  $U$  in the denominator of the integrand. The integral is defined only in regions of the flow where  $U'$  does not vanish, or to state it more precisely, where the parameter  $\frac{KU'}{U''}$  is large. Therefore, there exists a small region of size  $\frac{1}{K}$  around the maximum where the asymptotic expansion breaks down. In the outer region away from the extrema, we recover the expression (3) in the inertial limit  $\alpha \rightarrow 0$  first. For strictly monotonic velocity profiles  $U$ , we conclude that the inertial limit and the small scale forcing limit commute and that expression (3) is expected to be valid.

Using expression (3) for the Reynolds stress, we can solve Eq. (4) for the stationary profile. It writes

$$\frac{d}{dy} \left( \frac{\epsilon}{U'} \right) + U = 0. \quad (9)$$

Whatever the value of the free parameter  $U'(0)$ , all profiles  $U$  are diverging in finite length. An example of such a profile  $U$  is given in Fig. (2a). In red, we have plotted different solutions of Eq. (9) together such that the mean velocity profile  $U$  is composed of many diverging jets. In blue, we have drawn at hand what we expect qualitatively from a real velocity profile. An example of a real profile obtained by numerical simulations in [24] is displayed in Fig.(2b). The fact that Eq. (9) predicts diverging profiles  $U$  shows that the expression for the Reynolds stress (3) is not valid everywhere in the flow, but it holds only in the spatial subdomains where the flow is monotonic, not at the extrema. We observe that both divergences are regularized, by a cusp at the eastward jet maximum, and by a parabolic profile at the westward jet minimum. The second aim of this paper is to explain the asymmetric regularization of the eastward and westward jets.

Numerical simulations like the one performed in Fig. (2b) show that the mean velocity profile is regularized at a very small scale at its maximum. As we explained previously, there exists a region of typical size  $\frac{1}{K}$  around the maximum where the asymptotic expansion for the Reynolds stress breaks down. It is thus natural to choose the ansatz  $\tilde{U}(y) := U\left(\frac{y}{K}\right)$ . The scaling in  $\frac{1}{K}$  implies that the ratio  $\frac{U''}{K\alpha}$  is very large at the cusp because  $U'' \propto K^2$ . The cusp is then described by the inhomogeneous Rayleigh Eq. (8). If we put the ansatz  $\tilde{U}$  in (8) and consider the limit of large  $K$ , we get

$$\left( \frac{d^2}{dy^2} - \tan^2 \theta \right) \varphi_\delta(y, c) - \frac{\tilde{U}''(y)}{\tilde{U}(y) - c - i\delta} \varphi_\delta(y, c) = \frac{e^{i \sin \theta y}}{\tilde{U}(y) - c - i\delta}, \quad (10)$$

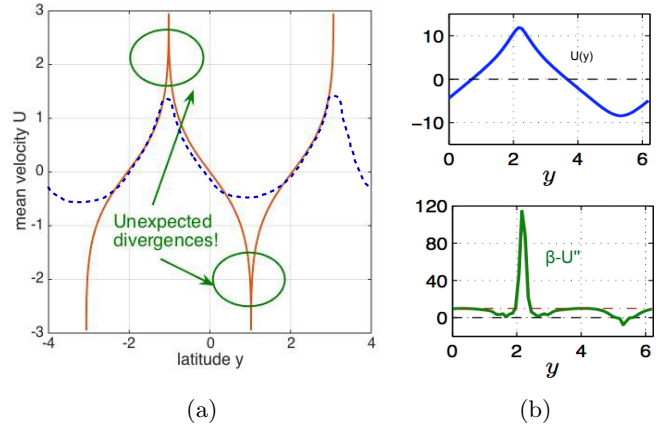


Fig. 2: (a) Jet profiles obtained as an analytic solution of (9) (red curve) together with a qualitative real velocity profile (blue curve). (b) Real velocity profile obtained in numerical simulations [24]. The analytic solution for  $U$  has divergences at the extrema that are regularized by a cusp at the eastward jet and a parabola at the westward jet.

where  $\cos \theta = \frac{k}{K}$ . The solution of this equation with  $\delta \rightarrow 0$  gives us the Laplace transform of the stream function with which we can express the Reynolds stress. The  $\beta$ -effect disappears completely from the equation of the cusp because in the region of the cusp, the curvature is so large that it overcomes completely the  $\beta$ -effect, as can be seen on the green curve of Fig. (2b). Eq. (10) together with the equations linking the Reynolds stress with  $\varphi$  have a numerical solution, which proves that our scaling  $\tilde{U}(y) := U\left(\frac{y}{K}\right)$  is self-consistent. This solution can not be expressed analytically and depends on the Fourier spectrum of the stochastic forcing. An example of a numerical integration of the Reynolds stress divergence  $-\partial_y \langle uv \rangle$  for the cusp is displayed in Fig. (3) for  $\tilde{U}(y) = -\frac{y^2}{2}$  and a stochastic forcing with a semi annular Fourier spectrum where  $\theta$  ranges between  $-\frac{\pi}{3}$  and  $\frac{\pi}{3}$ . In Fig. (3), the red curve is the asymptote  $\frac{\tilde{U}''}{\tilde{U}^2}$  obtained from formula (3) with  $\epsilon = 1$ . When a jet is in a stationary state, the cusp profile joins smoothly the outer region of the jet where the result (3) is valid.

Another physical phenomenon at the maximum of the jet is called “depletion at the stationary streamlines” and has first been observed in [23]. It means that at critical latitudes where  $U' = 0$ , any vorticity perturbation of the flow  $\omega_0$  has to asymptotically vanish with time. One main consequence of this phenomenon is the relation

$$U(y_{cr}) = -\frac{\epsilon K^2}{rU''(y_{cr})}, \quad (11)$$

where  $y_{cr}$  is the latitude of the extremum. From (11) we learn that, even if the velocity profile of the cusp depends on the details of the forcing, the maximal curvature of the profile satisfies a more general relation, and it would therefore be very interesting to check it in full numerical

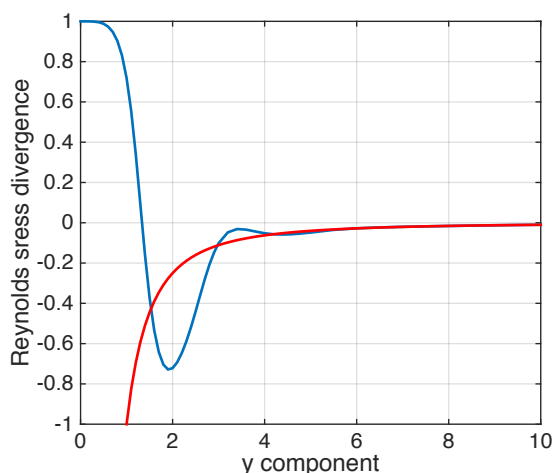


Fig. 3: The Reynolds stress divergence  $-\partial_y \langle uv \rangle$  (blue curve) computed for a parabolic profile  $\tilde{U}(y) = -\frac{y^2}{2}$  around its maximum  $y = 0$ . It is satisfying to observe that the red curve  $\frac{\tilde{U}''}{\tilde{U}^{1/2}}$  matches the blue curve for large  $y$  according to expression (3).

simulations with different types of forcing spectra.

256 The previous discussion successfully explained the jet  
 257 regularization of the eastward jet cusp. As clearly ob-  
 258 served in Fig. (2b), and from Jupiter data, westward jets  
 259 do not produce cusps. At first sight, it may seem that all  
 260 the theoretical arguments used so far, the energy balance,  
 261 the asymptotic expansions, and the results (3) and (11),  
 262 do not break the symmetry between eastward and west-  
 263 ward jets, as  $\beta$  disappears from all these computations.  
 264 However, as clearly stressed in [12], the whole theoretical  
 265 approach relies on an assumption of hydrodynamic stabil-  
 266 ity for  $U$ . The asymmetry is clearly visible in the Rayleigh-  
 267 Kuo criterion, that states that when  $\beta - U''$  change sign, an  
 268 instability may develop. We will now argue that the tur-  
 269 bulent flow is constantly oscillating between a stable and  
 270 unstable solution, in order to control the westward jet be-  
 271 havior. This means that the flow is not linearly stable, but  
 272 only marginally stable. As shown in the following, the in-  
 273 stability is localized at the extremum of the westward jet,  
 274 and the unstable mode has a very small spatial extension.  
 275 That's why the flow can be considered as stable away from  
 276 the westward extremum of the jet and the assumptions of  
 277 expression (3) are satisfied.

To check this marginal stability hypothesis, we solved numerically the homogeneous PDE for a perturbation carried by a mean flow

$$\partial_t \omega + ikU\omega + ik(\beta - U'')\psi = 0. \quad (12)$$

278 We chose a parabolic mean velocity with a small pertur-  
 279 bation at its minimum  $U(y) = \gamma \frac{y^2}{2} - \eta e^{-\frac{y^2}{\sigma^2}}$ . The main  
 280 curvature  $\gamma$  is chosen to be slightly smaller than  $\beta$ , and  
 281 we performed simulations using different values of  $\eta$  and  
 282  $\sigma$ . The result of one of those simulations is displayed in  
 283 figure (4). The red curve shows the Rayleigh-Kuo criterion

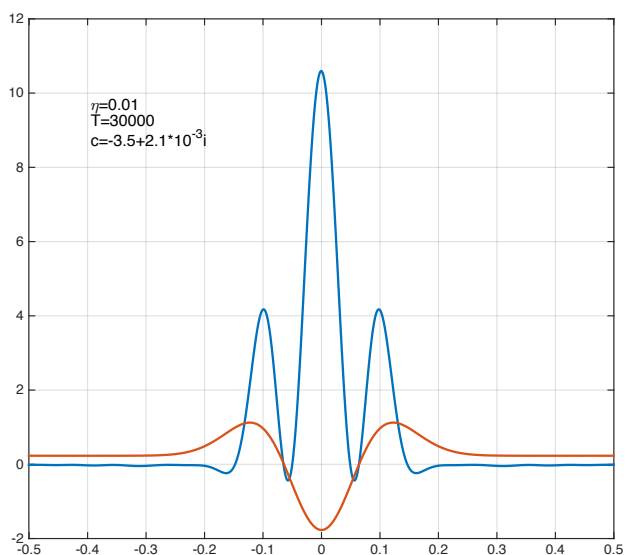


Fig. 4: Amplitude of the perturbation  $|\omega^2(y, t)| - 1$  (blue curve) carried by a mean flow  $U$ . The Rayleigh-Kuo criterion  $\beta - U''$  is displayed in red. The simulation shows that the perturbation grows exponentially with the complex rate  $c$ .

$\beta - U''$  which is locally violated around  $y = 0$ . The blue curve shows the amplitude of the perturbation  $|\omega^2(y, t)| - 1$  from which we can then express the Reynolds stress divergence. We check that the growth rate of the perturbation is indeed exponential with time with a complex rate  $c$ .

In this paper we gave a global consistent picture of how a zonal jet is sustained in a steady state through continuous energy transfer from small scale to large scale. Eq. (7) and (9) are probably the most striking results of this work, showing for the first time that it is possible to find closed equations for the velocity profile of turbulent flows. It illustrates that, although far from equilibrium, turbulent flow velocity profiles may be described by self consistent equations, as density of other macroscopic profiles can be described in condensed matter physics. This is a fundamental property which existence is far from obvious, and that no other approach was able to establish so far. In this paper, we have considered the case of a Rayleigh friction as the mechanism for removing energy that is transferred to the largest scale. Rayleigh friction is a rather ad-hoc type of damping (although it can be justified in certain cases involving, e.g., Ekman pumping). If one would consider other kinds of friction, for instance scale-selective damping, provided that this damping actually acts on the largest scales of the flow, in a corresponding inertial limit we expect most of our results to easily generalize (the proper dissipation operator should then replace Rayleigh friction in equation (4)). Indeed the processes that explain the computation of the Reynolds stress are inertial in nature and independent from the dissipation mechanisms. As an example, the case of viscous dissipa-

tion has been discussed in section 5.1.2 of [12], showing that while the regularization by viscosity is very different from the regularization by linear friction, the inertial results for the Reynolds stresses do coincide. This is true as far as the shear is non zero and equation (3) is concerned; by contrast the regularization of the cusp is dissipation dependent. In some specific cases, changing the dissipation mechanism may induce specific instability modes, like boundary layer modes due to viscous dissipation, however such effects are expected to be non generic. Extension and generalizations of our approach can be foreseen for other geometries (on the sphere), for more comprehensive quasi-geostrophic models of atmosphere jets, and for classes of flows dominated by a strong mean jet, for instance in some instances of boundary layer theory.

\* \* \*

We thank P. Ioannou for interesting discussion during the preliminary stage of this work. The research leading to these results has received funding from the European Research Council under the European Union's seventh Framework Program (FP7/2007-2013 Grant Agreement No. 616811).

## REFERENCES

- [1] L.D. Landau and E.M. Lifshitz. *Fluid Mechanics*. Number vol. 6. Elsevier Science, 2013.
- [2] S.B. Pope. *Turbulent flows*, 2001.
- [3] J. Paret and P. Tabeling. Experimental observation of the two-dimensional inverse energy cascade. *Physical review letters*, 79(21):4162, 1997.
- [4] J. Sommeria. Experimental study of the two-dimensional inverse energy cascade in a square box. *Journal of fluid mechanics*, 170:139–168, 1986.
- [5] DHE Dubin and TM ONeil. Two-dimensional guiding-center transport of a pure electron plasma. *Physical review letters*, 60(13):1286, 1988.
- [6] J.B. Marston, E. Conover, and T. Schneider. Statistics of an unstable barotropic jet from a cumulant expansion. *Journal of Atmospheric Sciences*, 65:1955, 2008.
- [7] P.H. Diamond, S.I. Itoh, K. Itoh, and T.S. Hahm. Zonal flows in plasma review. *Plasma Physics and Controlled Fusion*, 47(5):R35, 2005.
- [8] B. Galperin, R. Young, S. Sukoriansky, N. Dikovskaya, P. Read, A. Lancaster, and D. Armstrong. Cassini observations reveal a regime of zonostrophic macroturbulence on jupiter. *Icarus*, 229:295–320, 2014.
- [9] F. Bouchet and E. Simonnet. Random changes of flow topology in two-dimensional and geophysical turbulence. *Physical review letters*, 102(9), 094504, 2009.
- [10] A. Frishman, J. Laurie and G. Falkovich. Jets or vortices? What flows are generated by an inverse turbulent cascade? *Physical Review Fluids*, volume 2, 2017.
- [11] B. Farrell and P.Ioannou. Structural stability of turbulent jets. *Journal of the atmospheric sciences*, 60(17):2101–2118, 2003.
- [12] F. Bouchet, C. Nardini, and T. Tangarife. Kinetic theory of jet dynamics in the stochastic barotropic and 2d navier-stokes equations. *Journal of Statistical Physics*, 153(4):572–625, 2013.
- [13] J. Laurie, G. Boffetta, G. Falkovich, I. Kolokolov, and V. Lebedev. Universal profile of the vortex condensate in two-dimensional turbulence. *Physical review letters*, 113(25):254503, 2014.
- [14] G. Falkovich. Interaction between mean flow and turbulence in two dimensions. In *Proc. R. Soc. A*, volume 472, page 20160287. The Royal Society, 2016.
- [15] K. Srinivasan and WR Young. Reynolds stress and eddy diffusivity of  $\beta$ -plane shear flows. *Journal of the Atmospheric Sciences*, 71(6):2169–2185, 2014.
- [16] I. Kolokolov and V. Lebedev. Velocity statistics inside coherent vortices generated by the inverse cascade of 2d turbulence. *arXiv preprint arXiv:1609.00918*, 2016
- [17] I.Kolokolov and V. Lebedev. Structure of coherent vortices generated by the inverse cascade of two-dimensional turbulence in a finite box. *Physical Review E*, volume 93, 033104, 2016.
- [18] T.Tangarife. Kinetic theory and large deviations for the dynamics of geophysical flows. <https://tel.archives-ouvertes.fr/tel-01241523>, These Ecole normale supérieure de lyon, 2015.
- [19] C.Nardini and T. Tangarife. Fluctuations of large-scale jets in the stochastic 2D Euler equation. *arXiv:1602.06720*, 2016.
- [20] C.Porco, R.West, A.McEwen, A. Del Genio, A. Ingersoll, P. Thomas, S. Squyres, L. Dones, C. Murray, T. Johnson, et al. Cassini imaging of jupiter's atmosphere, satellites, and rings. *Science*, 299(5612):1541–1547, 2003.
- [21] Colette Salyk, Andrew P Ingersoll, Jean Lorre, Ashwin Vasavada, and Anthony D Del Genio. Interaction between eddies and mean flow in jupiter's atmosphere: Analysis of cassini imaging data. *Icarus*, 185(2):430–442, 2006.
- [22] F. Bouchet and E. Woillez. see supplement material available online for the computation of the reynolds stress divergence in the inertial small scale forcing limit. *EPL*, 2017.
- [23] F. Bouchet and H. Morita. Large time behavior and asymptotic stability of the 2D Euler and linearized Euler equations. *Physica D Nonlinear Phenomena*, 239:948–966, June 2010.
- [24] N. Constantinou. Formation of large-scale structures by turbulence in rotating planets. *arXiv preprint arXiv:1503.07644*, 2015.